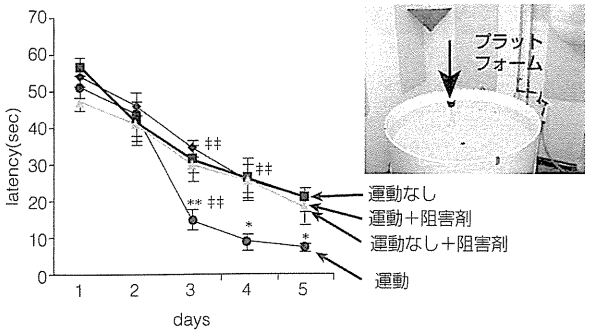

Vaynman, S., *et al.*: *Eur J Neurosci*, **20**, 2580-2590, (2004)

図2　自発走に伴う、認知機能(水迷路課題：写真参照)の改善
BDNFの受容体への結合を阻害すると、自発走(回転ホイール,7日)による認知機能改善効果が消失した.

身体運動がBDNFを介して認知機能(モリス水迷路課題：空間記憶獲得・保持)に及ぼす影響を検討した報告[11]がある(図2)。この研究では、身体運動に伴いマウスは周囲の環境を手掛かりに、プラットフォームに到達するまでの時間が短くなることが観察された。運動群では、顕著な学習記憶力の向上が認められるが、BDNF受容体への結合を阻害された運動群では、運動がもたらす認知機能向上効果が消失したことから、運動効果へのBDNFの部分的な関与が初めて確認された。

3. BDNFと抗うつ作用

BDNFとうつ病との関連性は、多くの動物実験、ヒトの死亡解剖、うつ病や抗うつ剤の効果の研究成果に基づいている。うつモデルラットの脳内BDNF含有量が低く、うつ治療後のラットの脳においてBDNF産生が増加することが報告されている。さらにヒトにおいても、うつ病患者の脳内BDNF濃度およびBDNFmRNA発現が低下しており[12]、自殺者やうつ患者の脳領域、特に海馬での遺伝子転写因子であるcAMP応答配列結合タンパク要素(cyclic-AMP response-element binding protein, CREB)BDNF、およびTrkB受容体のレベルが低下していることが観察されている[13]。

また、BDNF関連遺伝子関与において、ヒト型BDNFの前駆体(proBDNF)として合成され、プロアテーゼにより成熟BDNFには変換されるが、BDNFの遺伝子多型は成熟BDNFに存在しない。BDNFには66番目のバリンがメチオニンに置換する、多型(Val66Met)があることが知られている。このVal66Met型 は、エピソード記憶や海馬機能と関連していると考えられている[14]。さらに、Met型BDNFは動物実験によってBDNFの分泌を低下[15]、ヒトVal66Met多型とうつ病との関連性も報告されている[16]。これらの成果は、ヒトBDNFのVal66Met多型がBDNFの機能異常－分泌異常低下などをさせることによって、うつ病などの精神疾患を引き起こしている可能性を示唆しているが、大規模な研究によって、両者の関連性は認められていない[17]。しかし、最近の研究によりVal66MetでなくMet BDNF対立遺伝子がうつ患者の海馬の重量や自殺行動に関連することが報告された[18]。さらに、うつ病の発症と関連性があるとされる胎児期や発達期におけるストレスが、BDNFの発現やBDNF遺伝子を減弱させることから[19]、うつ病発症へのBDNF関連の遺伝子関与も否定できない。また、BDNFmRNA発現には、性差も確認されており、このような事実はうつ病発生の性差を示唆している。いずれにしても、うつ病の発症や病態の背景要因として、BDNF関与は重要な鍵となる可能性は否定できない。

うつ病患者では、血清BDNF水準が低下し、その水準はうつ病の重症度と負の相関を示すことや、うつ病患者のBDNF低下は抗うつ薬によって改善するとの知見もあることから、BDNF水準を高める方策はうつ病治療に繋がる可能性も示唆されている。

近年、運動によるうつ病予防・改善効果が報告されているが、ここでは抗うつ処置によるうつ病改善の類似性を考えてみたい。基礎と応用研究によれば、ストレスとうつはBDNFの発現や神経発生を減少させる。一方、抗うつ剤の処置はこれらの効果をブロックもしくは抑制し、うつ病の神経栄養因子仮説に導くだろうと考えられている。さらに、BDNF発現や神経発生は加齢に伴って減少し、うつ病発症の危険因子ともなっている。反対に、運動と豊かな環境は、神経栄養サポートと神経発生を増やし、ストレスや加齢の影響をブロックし、抗うつ作用をもたらす。

Duman[20]は、気分(感情)調節への神経栄養因子の関与に関する総説において，病態生理学的観点から以下のように要約している。

①ストレスとうつ病は神経栄養因子の活性を低下させ、ニューロンの萎縮および細胞損失をもたらす。
②うつ病患者のBDNF水準は低下している。
③ストレスは神経細胞新生を低下させる。
④ストレスとうつ病はニューロンの萎縮を引き起こす。
⑤海馬の重量はうつ病患者で低下している。

これらの現象をもたらす共通の背景として、糖質コルチコイドの関与が示唆されている。ヒトにおける研究では、尿中、唾液中および血清コルチゾール濃度の高値は、健常高齢者における将来の記憶機能の低下、認知機能や脳重量の低下、およびアルツハイマー病初期ステージの

認知機能の低下の予測因子であることが、疫学研究によっても確認されている。

さらにDumanら[21]は、抗うつ剤投与による臨床および実験的介入研究の成績から、以下のように結論を導いている。

①うつ処置は神経栄養因子の発現を高める。

②うつ処置は神経細胞新生を高める。

③抗うつ処置はストレスやうつ病の影響をブロックもしくは元に戻す。

④神経栄養因子はうつ病の行動モデルにおいて抗うつ作用を誘発する。

抗うつ剤投与の効果と類似して、運動はうつ病の薬物処置と同様に神経栄養因子/成長因子の発現と神経形成、神経発生を高め、抗うつ効果を誘発するようであるし、食事制限もまた神経栄養因子、神経発生および神経防御効果を有することが報告されている[21]。

おわりに

BDNFは、学習や記憶、情動に加え摂食、糖代謝などにおいても重要な働きをする分泌タンパク質であることを指摘した。特に、本稿では認知機能と抗うつ作用に関しては運動効果を含めて要約した。運動は様々な生活習慣病の発症予防・病態改善に有効に作用することは周知の事実であり[22]、そのメカニズムの一つとして、動物実験では、運動が脳や骨格筋におけるBDNF発現の増加をもたらすことが示唆された。さらに、ヒトにおける急性運動は血清BDNF水準を増加させることも示唆された。しかし、長期的な運動がBDNF水準に及ぼす影響や、急性運動による血清BDNF水準変動の意味については今後の検討課題であり、さらなる研究が期待されている[23]。

《《《《《 参考文献 》》》》》

1) Chen B, Dowlatshahi D, MacQueen GM, Wang JF, Young LT: Increased hippocampal BDNF immunoreactivity in subjects treated with antidepressant medication., *Biol Psychiatry.*, **50**, 260-265 (2001)

2) Phillips HS, Hains JM, Armanini M, Laramee GR, Johnson SA, Winslow JW: BDNF mRNA is decreased in the hippocampus of individuals with Alzheimer's disease., *Neuron*, **7**, 695-702 (1991)

3) Neeper SA, Gómez-Pinilla F, Choi J, Cotman CW: Physical activity increases mRNA for brain-derived neurotrophic factor and nerve growth factor in rat brain., *Brain Res*, **726**, 49-56 (1996)

4) Nakagawa T, Tsuchida A, Itakura Y, Nonomura T, Ono M, Hirota F, Inoue T, Nakayama C, Taiji M, Noguchi H: Brain-derived neurotrophic factor regulates glucose metabolism by modulating energy balance in diabetic mice., *Diabetes*, **49**, 436-444 (2000)

5) Radka SF, Holst PA, Fritsche M, Altar CA: Presence of brain-derived neurotrophic factor in brain and human and rat but not mouse serum detected by a sensitive and specific immunoassay., *Brain Res*, **709**, 122-301 (1996)

6) Pardridge WM, Kang YS, Buciak JL: Transport of human recombinant brain-derived neurotrophic factor (BDNF) through the rat blood-brain barrier in vivo using vector-mediated peptide drug delivery., *Pharm Res*, **11**, 738-746 (1994)

7) Hofer M, Pagliusi SR, Hohn A, Leibrock J, Barde YA: Regional distribution of brain-derived neurotrophic factor mRNA in the adult mouse brain., *EMBO J*, **9**, 2459-2464 (1990)

8) Linnarsson S, Björklund A, Ernfors P: Learning deficit in BDNF mutant mice., *Eur J Neurosci*, **9**, 2581-2587 (1997)

9) Kesslak JP, So V, Choi J, Cotman CW, Gomez-Pinilla F: Learning upregulates brain-derived neurotrophic factor messenger ribonucleic acid: a mechanism to facilitate encoding and circuit maintenance?, *Behav Neurosci*, **112**, 1012-1019 (1998)

10) Mu JS, Li WP, Yao ZB, Zhou XF: Deprivation of endogenous brain-derived neurotrophic factor results in impairment of spatial learning and memory in adult rats., *Brain Res*, **835**, 259-265 (1999)

11) Vaynman, S., Ying, Z. and Gomez-Pinilla, F.: Hippocampal BDNF mediates the efficacy of exercise on synaptic plasticity and cognition., *Eur J Neurosci*, **20**, 2580-2590 (2004)

12) Altar CA.: Neurotrophins and depression., *Trends Pharmacol Sci.*, **20**, 59-61 (1999)

13) Dwivedi Y, Rizavi HS, Conley RR, Roberts RC, Tamminga CA, Pandey GN.: Altered gene expression of brain-derived neurotrophic factor and receptor tyrosine kinase B in postmortem brain of suicide subjects., *Arch Gen Psychiatry*, **60**, 804-815 (2003)

14) Egan MF, Kojima M, Callicott JH, Goldberg TE, Kolachana BS, Bertolino A, Zaitsev E, Gold B, Goldman D, Dean M, Lu B, Weinberger DR.: The BDNF val66met polymorphism affects activity-dependent secretion of BDNF and human memory and hippocampal function.Cell, **112**, 144-145 (2003)

15) Chen ZY, Patel PD, Sant G, Meng CX, Teng KK, Hempstead BL, Lee FS:Variant brain-derived neurotrophic factor (BDNF) (Met66) alters the intracellular trafficking and activity-dependent secretion of wild-type BDNF in neurosecretory cells and cortical neurons., *J Neurosci*, **24**, 4401-4411(2004)
16) Strauss J, Barr CL, George CJ, Devlin B, Vetró A, Kiss E, Baji I, King N, Shaikh S, Lanktree M, Kovacs M, Kennedy JL: Brain-derived neuro- trophic factor variants are associated with childhood- onset mood disorder: confirmation in a Hungarian sample., *Mol Psychiatry*, **10**, 861-867 (2005)
17) Surtees PG, Wainwright NW, Willis-Owen SA, Sandhu MS, Luben R, Day NE, Flint J: No association between the BDNF Val66Met polymorphism and mood status in a non-clinical community sample of 7389 older adults., *J Psychiatr Res.*, **41**, 404-409 (2007)
18) Frodl T, Schüle C, Schmitt G, Born C, Baghai T, Zill P, Bottlender R, Rupprecht R, Bondy B, Reiser M, M_ller HJ, Meisenzahl EM: Association of the brain-derived neurotrophic factor Val66Met polymorphism with reduced hippocampal volumes in major depression., *Arch Gen Psychiatry*, **64**, 410-416 (2007)
19) Fujioka T, Fujioka A, Endoh H, Sakata Y, Furukawa S, Nakamura S: Materno-fetal coordination of stress-induced Fos expression in the hypothalamic paraventricular nucleus during pregnancy., *Neurosci*, **118**, 409-415 (2003)
20) Dunn, R: Neurotrophic factor and regulation of mood: Role of exercise, diet and metabolism., *Neurobiol Aging*, **26**(suppl.1), 88-93 (2005)
21) Dunn, W., Guo, Z., Jiang, H., Ware, M., and Mattoson, M.P.: Reversal of behavioral and metabolic abnormalities, and insulin resistance syndrome, by dietary restriction in mice deficient in brain-derived neurotrophic factor. Endcrinol, **144**, 2446-2453 (2003)
22) 熊谷秋三(責任編集): 健康と運動の疫学入門, 医学出版, 東京, (2009)
23) 野藤悠, 諏訪雅貴, 佐々木悠, 熊谷秋三: 脳由来神経栄養因子(BDNF)の役割と運動の影響, 健康科学, **31**, 49-59(2009)

くまがい・しゅうぞう／Shuzo Kumagai
九州大学基幹教育院、キャンパスライフ・健康支援センター
1979年　筑波大学大学院体育学研究科修士課程修了、1981年　佐賀医科大学助手、2003年　九州大学教授(健康科学センター)、2012年　九州大学健康科学センター長
専門・研究テーマ：健康・運動の疫学
最近の主な研究や活動：生活習慣病・介護予防に関する社会・運動疫学研究
著書・論文：Narazaki, K., Nofuji, Y., Honda, T., Matsuo, E., Yonemoto, K., and Kumagai, S.: Normative data for the Montreal Cognitive Assessment in a Japanese community-dwelling older population., Neuroepidemiol, **40**, 23-29(2013)
熊谷秋三：働きざかりの人のメンタルヘルスと運動．体育の科学，**63**, 17-21 (2013)
熊谷秋三(責任編集)：健康と運動の疫学入門．医学出版, (2008)

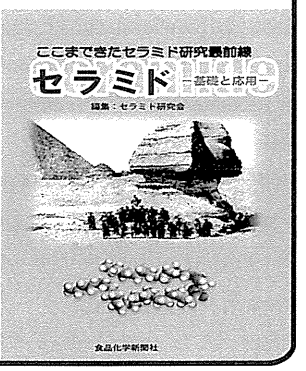

No.16

糖尿病がICD治療と死亡率におよぼす影響に関する検討

2014/1/27　　丸山 徹＝九州大学医学研究院病態修復内科学講座

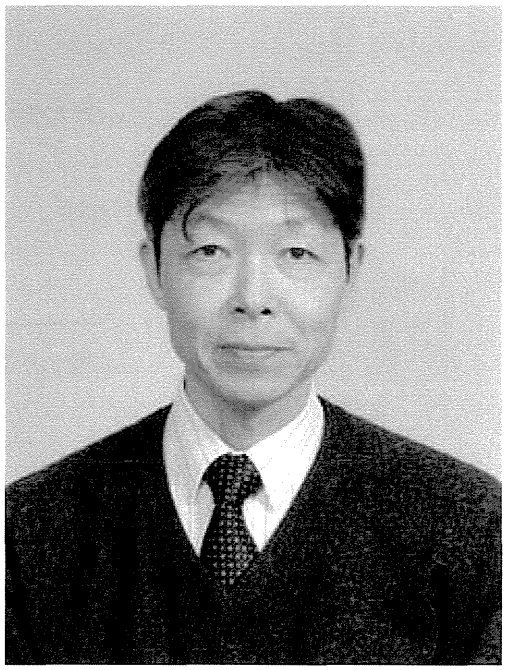

丸山徹氏

最新のICDプログラムは不適切作動を減らして死亡率を低下させることがMADIT-RITで明らかになった[1)]。一方、糖尿病はICD植え込み例でも心不全入院、心臓突然死、全死亡を増加させる[2)]。しかし糖尿病とICDの作動との関連は明らかではない。

【論文】

Influence of Diabetes Mellitus on Inappropriate and Appropriate Implantable Cardioverter-Defibrillator Therapy and Mortality in the Multicenter Automatic Defibrillator Implantation Trial-Reduce Inappropriate Therapy (MADIT-RIT) Trial. (Circulation 2013; 128: 694-701, DOI: 10.1161/CIRCULATIONAHA.113.002472)

【目的】

最新のICDプログラムが不適切作動や死亡率をいかに減らすか、それには糖尿病が影響するかを明らかにすること。

【対象】

Multicenter Automatic Defibrillator Implantation Trial-Reduce Inappropriate Therapy (MADIT-RIT) Trial[1)] に参加した1500人を対象とした。これらは一次予防でのICDまたはCRT-D植え込み例で、永続性心房細動、ペースメーカーなどの植え込み、3カ月以内の心筋梗塞や血行再建術後は除外した。糖尿病群は経口糖尿病治療薬の内服例とした。

【方法】

対象を3つのICDプログラム（図1）のいずれかに割り付け、適切または不適切作動と死亡をエンドポイントに平均17.4カ月追跡した。なお、作動は抗頻拍ペーシング（ATP）と電気ショック両方を含むとした。

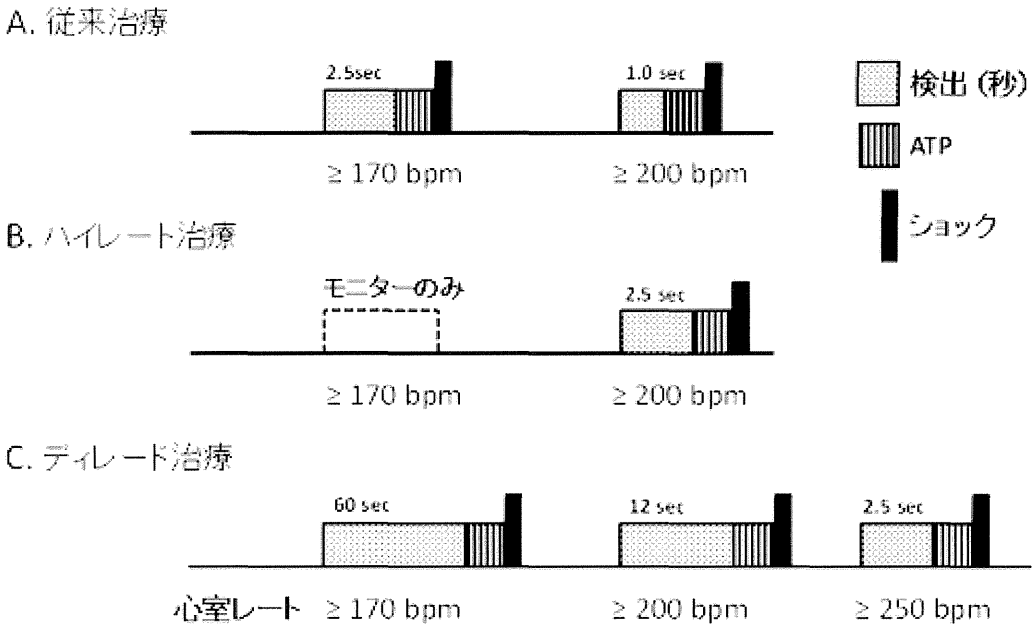

図1　ICDのプログラムの違いによる3種類の治療（BとCが最新治療）

【結果】

糖尿病は3つのICDプログラム間で均等に分布していた。糖尿病群には虚血性心筋症（64% vs. 48%）や高血圧（80% vs. 63%）が多く、安静時心拍数が高かった（73.3 vs. 71.5 bpm）。最新のICDプログラム（図1のBおよびC）は、糖尿病の有無に関係なく不適切作動を減少させた。

全てのICDプログラムで糖尿病群は不適切作動が少なく（図2のA）、Cox回帰分析では糖尿病はICDの不適切治療を46%減らし（P＝0.002）、その原因は不適切ショック（P＝0.44）ではなく不適切ATPの減少にあった（P＝0.002）。なお、不適切ATPの原因は心房細動や心房粗動ではなく、上室性頻拍と洞頻脈であった。一方、適切作動は糖尿病群で多かった（図2のB）。

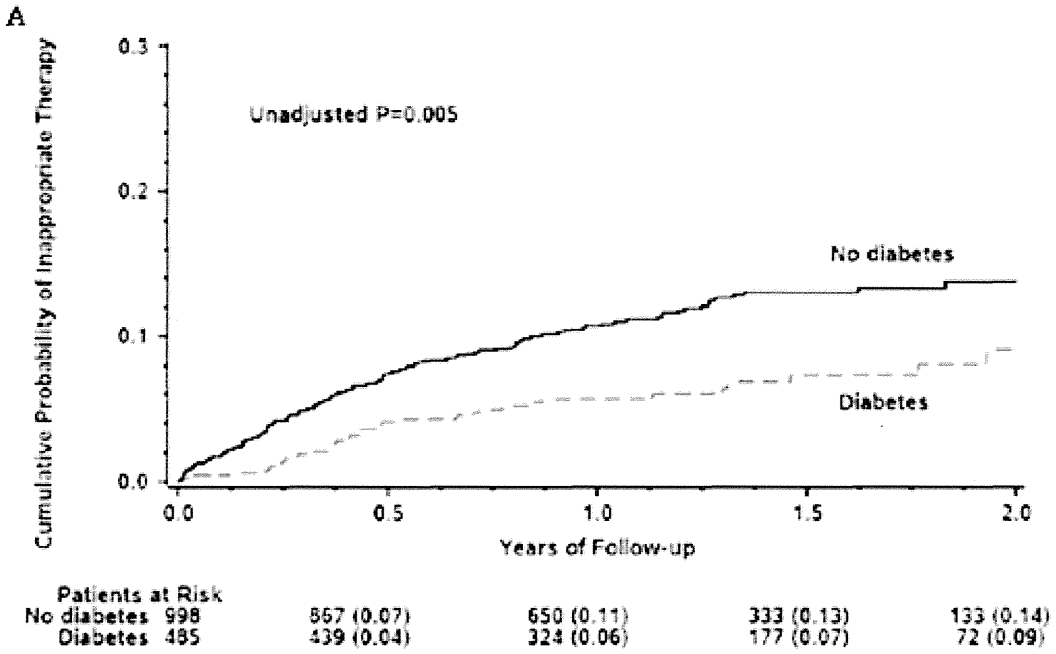

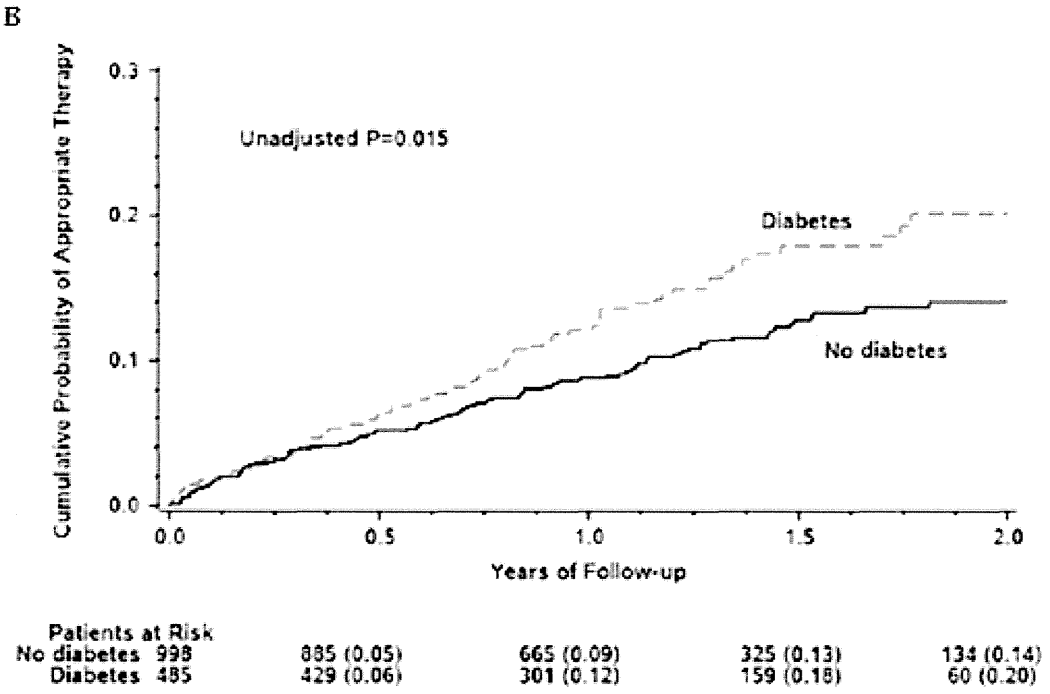

図2　糖尿病群と非糖尿病群のICD治療に関するカプランマイヤー曲線（A：不適切作動B：適切作動）[クリックで拡大]

ICD治療が死亡率におよぼす影響を糖尿病の有無で検討すると、糖尿病群でICD治療と死亡率との関連があり（表1）、不適切ショックは糖尿病の有無を問わず死亡率の上昇と関連していた。

表1　適切作動および不適切作動による糖尿病群と非糖尿病群の死亡リスク

	ハザード比	95%信頼区間	p値
糖尿病群			
不適切作動	4.17	1.52 – 11.40	0.005
適切作動	2.49	1.06 – 5.87	0.04
非糖尿病群			
不適切作動	1.63	0.60 – 4.41	0.34
適切作動	1.19	0.41 – 3.51	0.75

年齢、血圧、左室駆出率、心臓再同期療法の有無、NYHAクラス分類や虚血の重症度で補正したCox回帰モデル。

【結論】

最新のICDプログラムは不適切作動を減少させた。糖尿病群では上室性頻拍や洞頻脈による不適切ATPが少なかった。適切作動は糖尿病群で多く、また死亡率の増加に関連した。糖尿病心はICDやCRT-Dによる治療に対して脆弱であると言える。

ディスカッション

糖尿病は虚血性心臓病や心不全と関係し、ICD植え込み例にも多い。本研究は最新のICDプログラムが糖尿病例でも有用かを検証する目的で行われた。その結果、糖尿病群では不適切作動が少なく、その原因に自律神経障害で心拍数の急な上昇が起きにくい点が考えられた[3)]。他方、糖尿病群で適切作動が多く死亡率も高かったのは、糖尿病心の不整脈基質（虚血・線維化・瘢痕化）[4)]とICD治療に対する脆弱性を示している。

不全心ではICD治療の頻度が生命予後に直結する[5)]。このため糖尿病を合併するICD植え込み例では、予後改善のためプログラムの最適化が重要である。

■ 参考文献

1）Moss AJ, Schuger C, Beck CA, et al; MADIT-RIT Trial Investigators. Reduction in inappropriate therapy and mortality through ICD programming. N Engl J Med 2012; 367: 2275-2283.

2) Wittenberg SM, Cook JR, Hall WJ, et al; MADIT Trial. Comparison of efficacy of implanted cardioverter-defibrillator in patients with versus without diabetes mellitus.Am J Cardiol 2005; 96: 417-419.
3) Vinik AI, Ziegler D. Diabetic cardiovascular autonomic neuropathy. Circulation 2007; 115: 387-397.
4) Aneja A, Tang WH, Bansilal S, et al. Diabetic cardiomyopathy: insights into pathogenesis, diagnostic challenges, and therapeutic options. Am J Med 2008; 121: 748-757.
5) Poole JE, Johnson GW, Hellkamp AS, et al. Prognostic importance of defibrillator shocks in patients with heart failure.N Engl J Med 2008; 359: 1009-1017.

Original Contribution : MEMBRANE, 39 (1), 48-55 (2014)

Marked Impairment of Human Erythrocyte Filterability Caused by Oxidant Stress with AAPH Precedes Oxidative Hemolysis

Keita Odashiro [1], Toru Maruyama [2]*, Koichi Akashi [1],
Aya Sato [3], Shiro Mawatari [3], Takehiko Fujino [3]

1) Department of Medicine and Biosystemic Science, Kyushu University Graduate School of Medical Sciences
Fukuoka, Japan
2) Faculty of Art and Science, Kyushu University
Kasuga, Japan
3) Institute of Rheological Function of Foods Co. Ltd.
Hisayama, Japan

Erythrocytes as oxygen carriers are inevitably exposed to persistent oxidant stress, which determines in part the life span of circulating erythrocytes. Therefore, hemolytic and hemorheological effects of oxidant stress caused by 50 mM 2,2'-azobis(2-amidinopropane) dihydrochloride (AAPH) on intact human erythrocytes obtained from healthy volunteers (n = 6, mean age of 28.9 ± 10.3 years) were investigated. Incubation of erythrocyte suspension (3% in hematocrit) with 50 mM AAPH at 36 ℃ up to 3 hours increased the mean corpuscular volume of erythrocytes (from 83.0 ± 2.0 to 113.7 ± 2.5 fl finally, $p < 0.001$), and caused small but significant ($p < 0.001$) increases of methemoglobin (met-Hb) formation (5.8 ± 0.8%) and hemolysis to a final extent of 16.9 ± 2.8% in a time-dependent manner. Erythrocyte filterability (whole-cell deformability) was assessed by a highly sensitive and reproducible nickel mesh filtration technique, and defined as flow rate of erythrocyte suspension relative to that of saline (%) using the pressure-flow rate curve at a filtration pressure of 100 mmH_2O. Treatment with AAPH impaired the erythrocyte filterability in a time-dependent sigmoidal manner from 82.0 ± 1.2% to 12.0 ± 2.9%, which was pronounced 40 to 60 minutes after starting incubation. On the other hand, accelerated hemolysis was observed at least 60 minutes after starting exposure. These hematological and hemorheological findings indicate that oxidant stress caused by AAPH demonstrates time-dependent impairment of human erythrocyte filterability, erythrocyte swelling, met-Hb formation associated with chain-reacting erythrocyte membrane damage and resultant oxidative hemolysis. By simultaneous observations after starting oxidative stress, hemorheological impairment of erythrocyte behavior preceded the oxidative hemolysis. In this sense, erythrocyte filterability (whole-cell deformability), a prerequisite of microcirculation *in vivo*, is concluded to be a sensitive and clinically relevant parameter of oxidative erythrocyte damage leading to consequent hemolysis.

Key words : AAPH / erythrocytes / filterability / membrane / nickel mesh / oxidative stress

1. Introduction

Although reactive oxygen species (ROS), byproducts of biological oxygen consumption, correspond to only 0.1 to 0.2% of utilized oxygen, ROS play a key role in oxidative stress[1]. Oxidative stress involves various chronic health problems such as diabetes, cancer, senescence, and many circulatory disorders including atherosclerosis, hypertension, stroke and myocardial infarction. Microcirculation *in vivo* is also impaired by oxidative stress caused by ROS[2]. However, the mechanisms of this impairment are complicated at the cellular membrane, protein, lipid, and genome levels. Oxidative stress has a profound hemorheological impact on circulating erythrocytes. Erythrocytes are a major cellular component of circulating blood and a physiological oxygen carrier. Erythrocytes are also

* Corresponding Author
Tel: +81-92-583-7685
Fax: +81-92-592-2866
E-mail: maruyama@artsci.kyushu-u.ac.jp

sensitive to oxidant stress, because they are exposed to the redox (oxygenation/deoxygenation) cycle under intact *in vivo* circulation in spite of their intrinsic antioxidant defense mechanisms.

To date, many hemorheological methodologies have been established. However, these are diverse with different levels of sensitivity, specificity and reproducibility[3]. Moreover, the link between hemorheological and hematological derangements of erythrocytes exposed to an oxidative environment has not been fully investigated. Therefore, we assessed the hemorheological and hematological effects of oxidant stress caused by 2,2'-azobis(2-amidinopropane) dihydrochloride (AAPH) on human erythrocytes obtained from healthy volunteers, because AAPH is a small-molecular hydrophilic free radical initiator generating molecular nitrogen and 2 carbon radicals. This agent is currently used for investigations of biological lipid peroxidation and antioxidative potency of endogenous substances and exogenous food[4~6].

2. Experimental

2.1 Subjects

This study design was performed according to the Declaration of Helsinki (2000) and approved by the internal ethics committee of The Institute of Rheological Function of Foods Co. Ltd. (Hisayama, Fukuoka, Japan), with signed informed consent being obtained from subjects prior to enrollment in the study. Approximately 15 ml of venous blood was drawn from the antecubital vein of apparently healthy volunteers (n = 6, mean age of 28.9 ± 10.3 years) using 21-gauge needles and disposable evacuated syringes (Terumo Japan, Tokyo, Japan) containing EDTA-2Na or citrate-3Na as anticoagulants. Venous blood sampling was performed in the morning after an overnight fast.

2.2 Preparation of erythrocyte suspensions

Erythrocyte suspension was prepared as described elsewhere[7,8]. In brief, venous blood was centrifuged at 1300 × *g* for 10 minutes. Supernatant was carefully aspirated to replace buffy coat and plasma with saline buffered with N-(2-hydroxyethyl)-piperazine-N'-2-ethanesulfonic acid (HEPES) sodium salt (HEPES-NaOH). The composition of HEPES-NaOH-buffered saline was NaCl 141 mM and HEPES-NaOH 10 mM. Osmolality and pH of the HEPES-NaOH-buffered saline were 287 mOsm/kg·H_2O and 7.4, respectively. The osmolality of the HEPES-NaOH-buffered saline was measured using a freezing point depression-type osmometer (Fiske Mark 3 Osmometer, Fiske Associates, MA, USA). Erythrocytes were then washed three times at 4 ℃ by repeated re-suspension with HEPES-NaOH-buffered saline and centrifugation at 800 × *g*, 600 × *g* and 500 × *g* for 10 minutes each. The final hematocrit of human erythrocyte suspension was adjusted to 3.0%. These procedures were performed within 2 hours after blood sampling for subsequent experiments.

AAPH ($C_8H_{18}N_6 \cdot 2HCl$; MW = 271.2), a water-soluble radical generator of azo compound, was commercially obtained from Wako Pure Chem., Co. Ltd. (Osaka, Japan) and stored in a refrigerator at -20 ℃. The total volume of the reaction mixture was brought up to 5 ml by adding HEPES-NaOH-buffered saline. After preincubation at 36 ℃ for 5 minutes, the reaction was started by adding AAPH at a final concentration of 50 mM as in our previous study[9]. During this exposure, the mixture was incubated at 36 ℃ for the desired time period up to 3 hours. AAPH is so stable that the half-life of this agent is about 175 hours at 36 ℃ and at neutral pH, and that the rate of free radical generation is constant (rate of AAPH decomposition of 1.3×10^{-6} [AAPH]/sec) during the first several hours in reaction mixture[10]. Therefore, the reaction was terminated by cooling the test tubes in an ice bath, and the erythrocytes were pelleted by centrifugation at 1000 × *g* for 5 minutes at 4 ℃. Thereafter, AAPH-treated erythrocytes were washed twice and re-suspended with HEPES-NaOH-buffered saline.

2.3 Erythrocyte volume estimation

Blood cell counting and hematocrit measurements were carried out using a hemocytometer (Ace Counter, FLC-240A, Fukuda Denshi Co. Ltd., Tokyo, Japan). Mean corpuscular volume of erythrocytes (MCV; fl) was calculated automatically using this hemocytometer as a surrogate of average erythrocyte volume. After starting incubation with AAPH (50 mM) at 36 ℃, MCV was evaluated using re-suspension of AAPH-treated erythrocytes up to 3 hours after starting exposure. MCV estimation was performed at room temperature (22 ± 3 ℃). This parameter was also estimated in an erythrocyte suspension left for 3 hours without an exposure to AAPH.

2.4 Methemoglobin assay

An aliquot of the reaction mixture (0.4 ml) was hemolyzed using 5 ml of solution containing 100 mM phosphate buffer and 1% Triton X-100 (4:6 in volume ratio, pH 6.8) and then hemolysate was divided into two parts. The absorption peak at 630 nm of one part was read in the absence and presence of 5% potassium cyanide. The absorption peak of another part was read at 630 nm in the presence of 5% potassium ferricyanide and then read again at 630 nm after the addition of 5% potassium cyanide. The formation of methemoglobin (met-Hb, %) was calculated as previously reported[11]. Measurements were performed sequentially after starting exposure to 50 mM AAPH at 36 ℃, and these measurements were conducted at room temperature (22 ± 3 ℃).

2.5 Erythrocyte hemolysis assay

Erythrocyte suspension was subjected to exposure to 50 mM AAPH with different incubation times up to 3 hours. The reaction mixture was shaken gently at 36 ℃. At the desired interval, a small sample (400 μl) of reaction mixture was removed and diluted with 8 ml of HEPES-NaOH-buffered saline and centrifuged at 1000 × g for 5 minutes. Hemolysis was determined by the absorbance of hemoglobin at 540 nm in this supernatant[12 ~ 14]. Percent hemolysis (%) before and after starting incubation with AAPH was compared with complete hemolysis by treating the same erythrocyte suspension with distilled water. Hemolysis assay was performed at room temperature (22 ± 3 ℃).

2.6 Erythrocyte filterability measurement

Hemorheological equipment investigating erythrocyte filterability was introduced elsewhere[7, 8]. A nickel mesh filter was produced in accordance with our specifications by a photofabrication technique (Dainippon Printing Co. Ltd., Tokyo, Japan). We specified that this filter should have an outer diameter of 13 mm, a filtration area 8 mm in diameter, 11 μm thickness and with an interpore distance of 35 μm (Tsukasa Sokken Co. Ltd., Tokyo, Japan). The vertical and cylindrical pores were distributed regularly across the filter without coincidence or branching. The pore entrances exhibited round and smooth transition into the pore interior. Pore diameters were all exactly identical in a specific nickel mesh filter. Filters with a specific pore diameter ranging from 3 to 6 μm were available to be selected depending on the suspension materials. After repeating the preliminary experiments to choose an appropriate pore size, a nickel mesh filter with a pore diameter of 5.31 μm was chosen for human erythrocyte suspensions.

Filtration experiments were performed blindly using a gravity-based nickel mesh filtration apparatus (Model NOBU-II, Tsukasa Sokken Co. Ltd., Tokyo, Japan). In brief, the relationship between hydrostatic pressure (P; mmH_2O) and time (t; sec) was obtained during continuous filtration by gravity using a pressure transducer. P was transformed to a height of the meniscus in a vertical tube (h; mm). The tangent of the h-t curve determined by drawing points corresponding to different heights gives the rate of fall of the meniscus (dh/dt). Thereafter, by multiplying the rate of fall by the internal cross-sectional area of the vertical tube, the complete set of flow rates (Q; ml/minutes) and corresponding P, the P-Q relationship, was obtained[15, 16]. This procedure was automatically performed by measurement software installed in a personal computer (DELL Latitude CS, Dell Inc., Round Rock, TX, USA) and monitored on the main window of the computer screen. Together with the start of data acquisition, the measurement software displays the h-t curve continuously during the filtration process. When the filtration has been completed, the software displays the relationship of pressure and flow rate (P-Q curve). The h-t and P-Q curves are shown on the computer screen and stored simultaneously on Microsoft Office Excel 2003 in Windows XP (Microsoft, Tokyo, Japan). The temperature of the specimens was kept at 25 ℃ by circulating isothermal water through a water jacket surrounding the vertical tube. The percentage of the flow rate of erythrocyte suspension to that of HEPES-NaOH-buffered saline at 100 mm H_2O was used as an index of erythrocyte filterability. Filterability measurements were performed sequentially at the desired time after starting exposure to AAPH, and these measurements were conducted at room temperature (22 ± 3 ℃).

2.7 Data analyses

All data are expressed as means ± SD. Normality of the distribution of the hematological and hemorheological data was assessed by Kolmogorov-Smirnov test, and the demonstrated data were normally distributed.

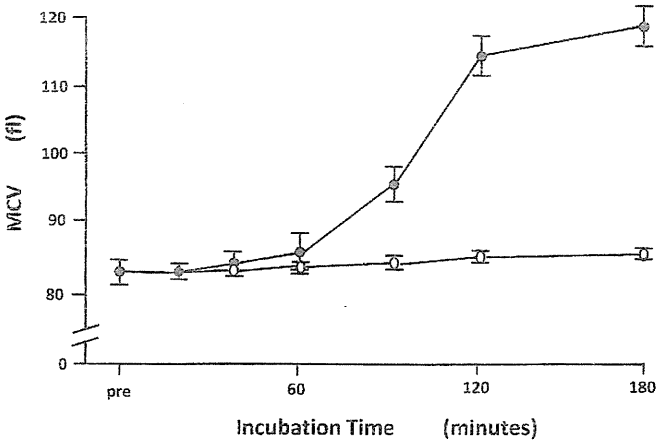

Fig. 1 Time-dependent changes of the mean corpuscular volume of erythrocytes (fl) with and without exposure to 50 mM AAPH (n = 6). Erythrocytes subjected to exposure to AAPH showed an increase in MCV, which was evident 60 minutes after the exposure (●). Erythrocytes without exposure to AAPH showed no changes in MCV (○). Symbols and bars indicate means ± SD. MCV, the mean corpuscular volume of erythrocytes (fl).

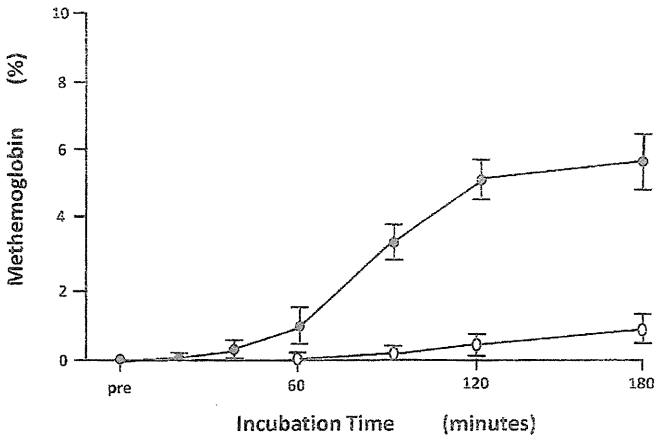

Fig. 2 Time-dependent changes of methemoglobin formation of erythrocytes (%) with and without exposure to 50 mM AAPH (n = 6). Erythrocytes subjected to exposure to AAPH showed time-dependent methemoglobin formation, which was evident 60 minutes after the exposure (●). Erythrocytes without exposure to AAPH showed negligible methemoglobin formation (○). Symbols and bars indicate means ± SD.

Therefore, time-dependent comparisons of these continuous variables were performed using the analysis of variance (ANOVA). Practical computation was performed using PASW (Predictive Analytics Software) on Windows version for Statistical Package of Social Science® (SPSS Inc., Chicago, Ill., USA). Differences with a two-sided $p < 0.050$ were considered significant.

3. Results

3.1 Erythrocyte volume estimation

Fig. 1 shows MCV as a function of time of an exposure of erythrocyte suspension to AAPH (50 mM). The MCV at preincubation was 83.0 ± 2.0 fl (means ± SD). The MCV significantly increased in a time-dependent manner ($n = 6$, $p < 0.001$), indicating erythrocyte swelling caused by AAPH-induced oxidant stress. This phenomenon was accelerated an hour after starting exposure to AAPH, and the final MCV of erythrocyte suspension under 3 hours of incubation was 113.7 ± 2.5 fl (means ± SD). On the other hand, the MCV of erythrocyte suspension left for 3 hours after preparation without AAPH exposure was equivalent to that of preincubation (83.1 ± 2.4 fl, means ± SD).

3.2 Methemoglobin assay

The AAPH-treated erythrocyte suspension exhibited a slightly dark brownish color in a time-dependent manner. Spectrophotometric analysis demonstrated the formation of met-Hb with an absorption peak at 630 nm. After 3 hours of treatment with AAPH, this agent revealed a small but significant ($p < 0.001$) increase of met-Hb ranging from 5.0 to 6.5% ($n = 6$, 5.8 ± 0.8%, means ± SD), whereas the met-Hb formation at preincubation was not detectable at all (Fig. 2). This increase of met-Hb of erythrocyte suspension at the end of exposure was also significant ($n = 6$, $p < 0.001$) compared with met-Hb levels left for 3 hours without AAPH treatment (1.2 ± 0.5%, means ± SD), indicating AAPH-triggered auto-oxidation of oxyhemoglobin.

3.3 Erythrocyte hemolysis assay

Fig. 3 shows a hemolytic time course obtained by an exposure of erythrocyte suspension to 50 mM AAPH. Incubation of erythrocytes with AAPH yielded hemolysis in a time-dependent manner, that is progression of hemolysis ranging from 6.3 to 9.8% ($n = 6$, 7.9 ± 1.8%, means ± SD) was observed 90 minutes after starting incubation, and 14.3 to 19.9% ($n = 6$, 16.9 ± 2.8%, means ± SD) hemolysis at 3 hours of exposure. Erythrocyte suspension left for 3 hours without expo-

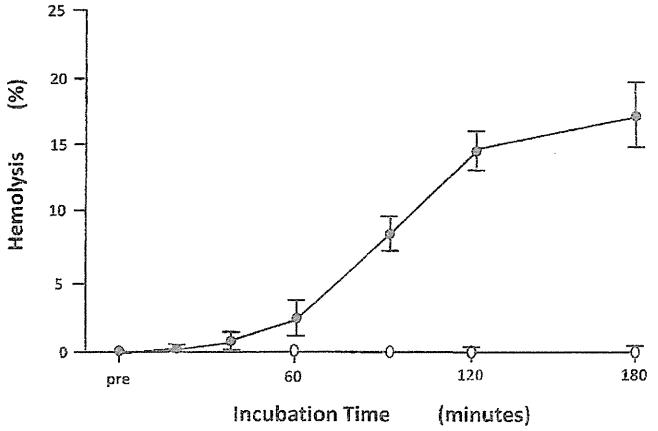

Fig. 3 Hemolytic time course of erythrocyte suspension (%) exposed to 50 mM AAPH (n = 6). Erythrocytes subjected to exposure to AAPH showed time-dependent hemolysis, which was evident 60 minutes after starting the exposure (●). Erythrocyte suspension without exposure to AAPH showed no evident hemolysis (○). Symbols and bars indicate means ± SD.

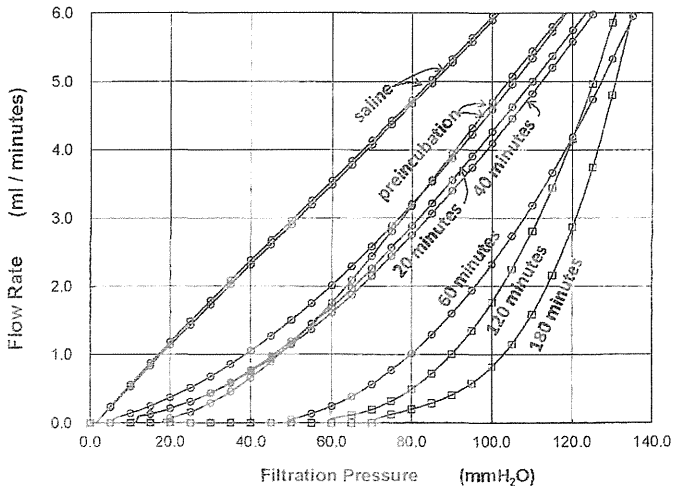

Fig. 4 Representative relationships between filtration pressure (P; mmH_2O) and flow rate (Q; ml/minutes) during continuous filtration experiment using HEPES–NaOH–buffered control saline and human erythrocyte suspensions obtained from healthy volunteers (n = 6). The P–Q relationships correspond to two control saline passages, passages of erythrocyte suspensions in preincubation and under incubation with 50 mM AAPH at incubation times of 20, 40, 60, 120 and 180 minutes.

sure to AAPH displayed no evident hemolysis at all.

3.4 Erythrocyte filterability measurement

Fig. 4 indicates the results of representative filtration experiments. The pressure vs. flow rate relationship of

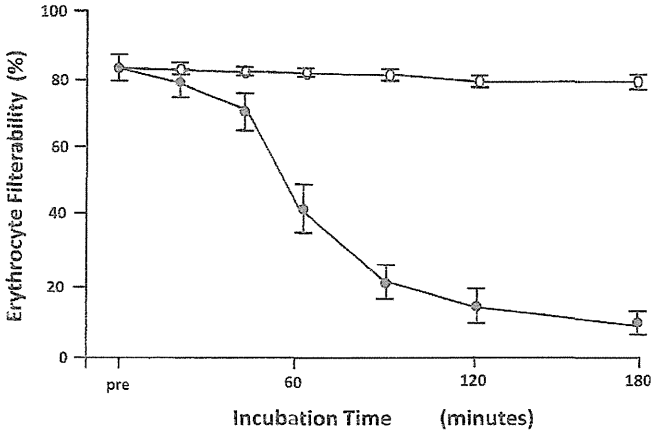

Fig. 5 Summarized data of continuous filtration experiments (n = 6). Filterability of human erythrocyte suspensions exposed to 50 mM AAPH showed time-dependent reduction, which was marked at incubation times of 40 to 60 minutes after starting exposure (●), whereas the filterability of erythrocyte suspension without exposure to AAPH remained at the preincubation levels (○). Symbols and bars indicate means ± SD.

control HEPES–NaOH–buffered saline shows a straight line passing through the origin, indicating that saline is Newtonian fluid. Filtration of control saline displayed a completely superimposable pressure–flow line, indicating that this filtration system satisfies the reproducibility. Suspension of erythrocytes obtained from different volunteers prior to an exposure to AAPH produced a concave curve showing that the erythrocyte suspension *per se* is originally not Newtonian. Moreover, pressure–flow curves of the control erythrocyte suspension were considerably superimposable, implying that the normal range of erythrocyte filterability estimated by this technique is quite limited. Treatment with AAPH (50 mM) decreased the flow rate of erythrocyte suspension at any given filtration pressure. These phenomena were evident in a time–dependent manner, that is, the flow–pressure curves shifted gradually to the right according to the progression of exposure to AAPH. Erythrocyte filterability was determined as flow rate of erythrocyte suspension relative to that of saline at 100 mmH_2O (%).

Fig. 5 shows the summarized data of filterability of erythrocyte suspension before and after the treatment with AAPH. Average erythrocyte filterability prior to the treatment was 82.0 ± 1.2% (means ± SD), and the final filterability 3 hours after starting the treatment was 12.0 ± 2.9% (means ± SD). This agent therefore

impaired the erythrocyte filterability progressively in a time-dependent sigmoidal manner ($n = 6$, $p < 0.001$). The impairment of erythrocyte filterability was marked during incubation times ranging from 40 minutes to 60 minutes after starting exposure to AAPH. The filterability of the erythrocyte suspension 3 hours after the preparation without an exposure to AAPH was equivalent to that of preincubation (80.1 ± 1.6%, means ± SD).

4. Discussion

Circulating erythrocytes as an oxygen carrier exposed to periodic high oxygen pressure are a main cellular target of *in vivo* oxidative stress. Therefore, it is of interest to assess hemorheological and hematological correlations of intact human erythrocytes exposed to AAPH, which is used widely as an oxidative stress model at the cellular level[12 ~ 14, 17]. AAPH acts as an alkyl radical initiator at physiological temperature. In our laboratory, the biochemical effects of oxidative injury caused by AAPH (50 mM) on the isolated human erythrocyte membrane have been investigated[9]. Hemolysis is the final event in the disposal of damaged erythrocytes with impaired deformability, and the mechanisms of hemolysis in AAPH-exposed erythrocytes are not fully understood. Therefore, this study was performed in this oxidant stress model using our hemorheological method.

The filterability of erythrocytes that pass through the microvascular network is an essential factor affecting physiological microcirculation. Since *in vivo* erythrocyte deformation involves bending, a filtration technique is a promising tool of hemorheology in that erythrocyte filterability is considered as whole-cell bending deformability[15, 16]. The evaluation of filterability strictly depends on the measurement technique, and the nickel mesh filtration technique is highly sensitive, quantitative and reproducible by assessing the physiological bending deformation of intact erythrocytes[18 ~ 20]. As a matter of fact, the present study demonstrated clearly that the normal filterability of human erythrocytes was quite limited to pretty narrow range around 80%, the filterability of erythrocytes exposed to 50 mM AAPH is dramatically impaired, and this impairment is accelerated 40 to 60 minutes after starting incubation (Fig. 5). By incubation for 3 hours, AAPH impaired the filterability so much that no-flow was observed under the filtration pressure of 70 mmH_2O or less (Fig. 4), indicating that AAPH-damaged erythrocytes were stuck in the nickel mesh pores.

In the present study, MCV of erythrocytes exposed to 50 mM AAPH was increased in a time-dependent manner (Fig. 1), indicating that AAPH-induced oxidative stress caused gradual erythrocyte swelling. When the thickness of swollen erythrocytes increases, disc-like erythrocytes' bending deformation inevitably becomes difficult, leading to time-dependent impairment of the filterability (Figs. 4 and 5). AAPH-induced oxidative stress increases erythrocyte membrane permeability for water and small ions such as K^+ [21] and Ca^{2+} [17]. This is supposed to be due to AAPH-induced progressive membrane phospholipid peroxidation and membrane leakage formation, because the time-dependent degradation of membrane phospholipid was confirmed in our previous study, that is 50 mM AAPH dramatically reduced α-tocopherol and γ-tocopherol to less than 50% and phosphatidylethanolamine to 80% of their initial levels[9]. On the other hand, band 3 protein plays an important role in cellular volume regulation as an anion exchanger, and is considered to be another target of AAPH-induced oxidative stress[22, 23].

The met-Hb formation as observed in this study (Fig. 2) indicates the interaction of AAPH liberating ROS with oxyhemoglobin and oxidation of the heme iron. This phenomenon is confirmed in the oxidant stress model of human erythrocytes using hypoxanthine-xanthine oxidase reaction generating superoxide anion. However, the application of superoxide to the resealed ghost of human erythrocytes did not cause any discernible membrane damage[24]. This strongly indicates that intracellular met-Hb formation yields chain-reacting auto-oxidation of membrane components such as membrane protein degradation and membrane phospholipid peroxidation leading to membrane leakage and cellular swelling. Comparatively, percent met-Hb formation induced by lipophilic peroxidant *tert*-butylhydroperoxide (nearly 60%)[11] is far greater than that induced by this hydrophilic AAPH (less than 10%) under different (0.5 mM vs. 50 mM) but equivalent doses with respect to the extent of hemolysis[13, 14, 25]. This supports the assertion that the different membrane permeabilities and hence different locations of ROS generation between *tert*-butylhydroperoxide and AAPH underlie the different extents of met-Hb formation[23]. Because hydrophobicity of a

drug influences its penetration of erythrocyte membrane or its location within the membrane phospholipid organization.

Erythrocyte swelling impairs the filterability (whole-cell bending deformability) by reducing the ratio of surface area to its volume. Oxidatively damaged erythrocytes cause K^+ efflux which may allow concomitant water efflux. This may counteract the swelling of AAPH-treated erythrocytes. However, such membrane damage also allows Ca^{2+} and Na^+ influx that balance the K^+ efflux. Therefore, there seems to be no changes of the intracellular total cation content in the oxidatively damaged erythrocytes[26]. We speculate the membrane leak pathway other than ion-permeable channels, i.e., prelytic pores in the perturbed membrane may play a role in water influx and erythrocyte swelling. Scanning electron microscopic examination clarified gross morphological changes of membrane blebs, extrusions and ruffling in the AAPH-treated erythrocytes, suggesting nonspecific water-permeable leak pathway[14].

An AAPH-evoked, time-dependent hemolysis was observed (Fig. 3) as in previous studies that applied the same concentration of AAPH (50 mM) to the human erythrocyte suspension with hematocrit ranging from 5 to 10% that is slightly higher than in this study (3%) [13, 14]. Oxidative hemolysis is a final event of extremely damaged erythrocytes, which was evident hemorheologically in this study (Fig. 4). As a matter of fact, AAPH-induced hemolysis is preceded by the markedly impaired filterability (Figs. 3 and 5). Human organisms possess several antioxidant defense mechanisms such as membrane α-tocopherol, internal enzymes such as catalase, superoxide dismutase and glutathione peroxidase. Lag of erythrocyte swelling (Fig. 1), met-Hb formation (Fig. 2), impairment of filterability (Fig. 5) and hemolysis (Fig. 3) after starting the application of AAPH may reflect the redox reaction of the defense system against extrinsic oxidant stress[14].

This study has several limitations. First, hemolysis assay was performed in reaction mixture under static condition without any shear stress, and is not directly correlated to dynamic erythrocyte filterability. In that filtration process *per se* induces mechanical stress, the combined mechanical and oxidative stress may accelerate the erythrocyte damage which promotes hemolysis to a greater extent than that observed in the present study[26]. The second limitation is a lack of osmotic control in the reaction mixture of incubation with AAPH. However, AAPH-induced increase of MCV indicates that oxidative effects predominate over osmotic effects. The third limitation is that the reasons for the erythrocyte filterability impairment preceding the erythrocyte swelling remain unclear. More comprehensive protocol including erythrocyte oxidation such as malondialdehyde quantification is required to answer this question. Moreover, such mechanistic membrane study should include electron microscopic and fluorescent polarization techniques to investigate oxidatively damaged membrane structure and fluidity.

5. Conclusions

The present study indicates that oxidant stress induced by AAPH demonstrates time-dependent impairment of human erythrocyte deformability, erythrocyte swelling and met-Hb formation leading to oxidative hemolysis. This series of oxidative events are considered to be interdependent. Erythrocyte swelling causes geometric influences, and met-Hb induces chain-reacting oxidative membrane damage. These combined effects accelerate the impairment of AAPH-treated erythrocyte deformability. Our filtration technique clarified that hemorheological derangement precedes the oxidative hemolysis, which is relevant to *in vivo* microcirculation observed in vigorous athletes and subjects with unstable hemoglobin[27, 28]. However, prime factors initiating this hemorheological derangement remain unknown in this study.

Acknowledgements

The authors would like to thank the staff of the Institute of Rheological Function of Foods Co. Ltd. (Hisayama, Fukuoka) for technical assistance. We lost our collaborator, Dr. Nobuhiro Uyesaka (Department of Physiology, Nippon Medical University), during the preparation of this manuscript, and dedicate this work to honor his memory.

References

1) Tahara EB, Navarete FD, Kowaltowski AJ : *Free Radic. Biol. Med.*, **46**, 1283-1297 (2009)
2) Crimi E, Ignarro LJ, Napoli C : *Free Radic. Res.*, **41**, 1364-1375 (2007)
3) Caimi G, Presti RL : *Acta Diabetol.*, **41**, 99-103 (2004)
4) Asikin Y, Takahashi M, Mishima T, Mizu M, Takara K,

Wada K : *Food Chem.*, **141**, 466-472 (2013)
5) Zhang D, Xie L, Wei Y, Liu Y, Jia G, Zhou F, Ji B : *Food Chem.*, **141**, 347-356 (2013)
6) Rosenblat M, Elias A, Volkova N, Aviram M : *Free Radic. Res.*, **47**, 257-267 (2013)
7) Ariyoshi K, Maruyama T, Odashiro K, Akashi K, Fujino T, Uyesaka N : *Circ. J.*, **74**, 129-136 (2010)
8) Ejima J, Ijichi T, Ohnishi Y, Maruyama T, Kaji Y, Kanaya S, Fujino T, Uyesaka N, Ohmura T : *Clin. Hemorheol. Microcirc.*, **22**, 1-7 (2000)
9) Mawatari S, Saito K, Murakami K, Fujino T : *Metabolism*, **53**, 123-127 (2004)
10) Niki E : *Methods Enzymol.*, **186**, 100-108 (1990)
11) Okamoto K, Maruyama T, Kaji Y, Harada M, Mawatari S, Fujino T, Uyesaka N : *Jpn. J. Physiol.*, **54**, 39-46 (2004)
12) Sato Y, Kamo S, Takahashi T, Suzuki Y : *Biochemistry*, **34**, 8940-8949 (1995)
13) Dai F, Miao Q, Zhou B, Yang L, Liu ZL : *Life Sci.*, **78**, 2488-2493 (2006)
14) Wang J, Sun B, Cao Y, Tian Y : *Food Chem. Toxicol.*, **47**, 1591-1599 (2009)
15) Arai K, Iino M, Shio H, Uyesaka N : *Biorheology*, **27**, 47-65 (1990)
16) Nakamura T, Hasegawa S, Shio H, Uyesaka N : *Blood Cells*, **20**, 151-165 (1994)
17) Quintanar-Escorza MA, González-Martinez MT, del Pilar IO, Calderón-Salinas JV : *Toxicol. In Vitro*, **24**, 1338-1346 (2010)
18) Rodgers GP, Dover GJ, Uyesaka N, Noguchi CT, Schechter AN, Nienhuis AW : *N. Engl. J. Med.*, **328**, 73-80 (1993)
19) Hiruma H. Noguchi CT, Uyesaka N, Schechter AN, Rodgers GP : *Am. J. Physiol.*, **268**, H2003-H2008 (1995)
20) Oonishi T, Sakashita K, Uyesaka N : *Am. J. Physiol.*, **273**, C1828-C1834 (1997)
21) Banerjee A, Kunwar A, Mishra B, Priyadarsini KI : *Chem. Biol. Interact.*, **174**, 134-139 (2008)
22) Celedón G, González G, Ferrer V, Lissi EA : *Free Radic. Res.*, **38**, 1055-1059 (2004)
23) Celedón G, González G, Lissi EA, Hidalgo G: *IUBMB Life*, **51**, 377-380 (2001)
24) Uyesaka N, Hasegawa S, Ishioka N, Ishioka R, Shio H, Schechter AN : *Biorheology*, **29**, 217-229 (1992)
25) Albertini MC, Ghibelli L, Ricciotti R, Fumelli C, Canestrari F, Galli F, Rovidati S, Bonanno E, Fumelli P : *Arch. Gerontol. Geriatr.*, **22** (suppl. 1), 423-428 (1996)
26) Ney PA, Christopher MM, Hebbel RP : *Blood*, **75**, 1192-1198 (1990)
27) Smith JA : *Sports Med.*, **19**, 9-31 (1995)
28) Winterbourn CC : *Semin. Hematol.*, **27**, 41-50 (1990)

(Received 23 September 2013 ;
Accepted 2 December 2013)

JAFIB
Original Research
Journal of Atrial Fibrillation

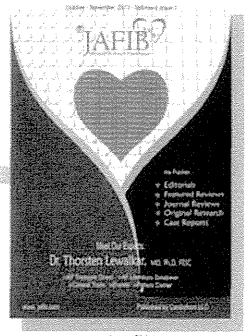

www. jafib.com

Impaired Erythrocyte Deformability in Patients with Coronary Risk Factors: Significance of Nonvalvular Atrial Fibrillation

Keita Odashiro, MD[1], Toru Maruyama, MD[2], Taku Yokoyama, MD[1], Hisataka Nakamura, MD[1], Mitsuhiro Fukata, MD[1], Shioto Yasuda, MD[1], Kazuyuki Saito, MD[3], Takehiko Fujino, MD[4], and Koichi Akashi, MD[1]

[1]Department of Medicine, and [2]Faculty of Art and Science, Kyushu University, [3]BOOCS Clinic, [4]Institute of Rheological Function of Foods Co. Ltd., Fukuoka, Japan.

Abstract

Although coronary risk factors promote the formation of atherosclerotic plaque containing activated platelets and inflammatory leukocytes, and play a pivotal role in the development of coronary artery diseases (CAD), the hemorheological effects of these risk factors on circulating intact erythrocytes, a major component of whole blood cells, are poorly understood. Therefore, this study aimed to quantify erythrocyte deformability in patients with coronary risk factors, and enrolled 320 consecutive cardiac outpatients including 33 patients with nonvalvular atrial fibrillation (AF). Patients with acute coronary syndrome or valvular AF were excluded. Demographic variables obtained by medical records were correlated with erythrocyte deformability investigated by our highly sensitive and reproducible filtration technique. Among demographic variables, triglyceride ($p = 0.004$), HbA1c ($p = 0.014$) and body weight ($p = 0.020$) showed significant inverse correlation to the erythrocyte deformability. This deformability was not associated with types of CAD (old myocardial infarction vs. stable angina) or modality of treatment (percutaneous intervention vs. coronary artery bypass grafting). Unexpectedly, stepwise multiple regression analysis demonstrated that nonvalvular AF was the most significant contributor to the impaired erythrocyte deformability ($p = 0.002$). Hypertension and dyslipidemia are more prevalent in the AF patients ($p < 0.001$), and the erythrocyte deformability was found to be impaired synergistically and significantly ($p < 0.001$) during the stepwise accumulation of the coronary risk factors in addition to AF. In conclusion coronary risk factors synergistically impair the erythrocyte deformability, which may play an important role in critically stenotic coronary arteries. Since the impairment of intact erythrocyte deformability is mostly associated with nonvalvular AF, this common arrhythmia may reflect the coronary risk accumulation.

Introduction

Hemorheology in association with coronary atherosclerotic plaque formation has drawing increasing attention. Much effort has been devoted to elucidate the role of activated platelets and leukocyte (scavenger macrophages, activated lymphocytes and inflammatory polymorphonuclear neutrophils) in atherosclerotic progression and prothrombotic tendencies. In contrast, the effects of coronary risk factors on the behaviors of circulating intact erythrocytes, major component of whole blood cells, have been poorly understood in actual cardiac patients. The deformability of erythrocytes that pass through the microvascular network is an essential factor to maintain the physiological fluent microcirculation. Physiological and hematological values of erythrocyte deformability are equivalent to those of platelet aggregating and leukocyte migratory functions. However, the concept of erythrocyte deformability has not been strictly defined as a physical quantity, and the evaluation of deformability depends on the measurement technique and its relative sensitivity.[1] Erythrocytes deformability is supposed to be impaired in patients with coronary artery disease (CAD) by mechanical stress depending on plaque morphology such as irregular surface, calcified plaque edge and sharp plaque shoulder. This deformability is also impaired by shear stress of high blood flow velocity observed in stenotic coronary arteries. Nevertheless, erythrocytes deformability is a fundamental prerequisite of coronary microcirculation maintaining patency of critically stenotic coronary arteries or collateral circulation.[2] Therefore, the aim of this study is to investigate the homerheologic effects of coronary risk factors on the intact erythrocyte deformability, using our highly sensitive and reproducible filtration technique. In this setting, erythrocyte

Key Words:
Atrial fibrillation, Coronary risk factors, Deformability, Erythrocytes

Disclosures:
Done.

Corresponding Author:
Toru Maruyama, MD., PhD.
Faculty of Art and Science
Kyushu University
Kasuga Kohen 6-1, Kasuga 816-8580
Japan.

deformability is considered as filterability of erythrocyte suspension. As mMicropipette technique, a representative hemorheologic methods other than filtration technique, estimates single erythrocyte membrane rigidity, one of the components regulating whole cell deformability.[3] Therefore, erythrocyte suspension filterability is considered as whole cell deformabilty.

Methods

Study Population

This study was approved by the internal ethics committee of the Institute of Rheological Function of Foods Co. Ltd. (Fukuoka, Japan) and was performed in accordance with the Declaration of Helsinki, i.e., signed informed consent was obtained from each subject prior to enrollment into the study. The study population consisted of 320 Japanese patients (209 males and 111 females) with common cardiac and/or systemic diseases. All patients were managed monthly at least over 1.5 years and treated at the discretion of attending physicians in the outpatients section of the Kyushu University Hospital (Fukuoka, Japan) or in several teaching hospitals and community clinics affiliated to the University Hospital. Hypertension was defined as casual blood pressure > 140/90 mmHg or treatment with antihypertensive drugs. Type 2 diabetes mellitus was defined as fasting serum glucose > 126 mg/dl, casual serum glucose > 200 mg/dl, HbA1c(NGSP) > 6.5% and/or current antidiabetic medication.4 Patients with type 1 diabetes mellitus were not enrolled. Dyslipidemia was defined as serum LDL cholesterol > 140 mg/dl, serum HDL cholesterol < 40 mg/dl or prescription of lipid-lowering agents.[4] Coronary artery disease (CAD) included old myocardial infarction and stable angina pectoris irrespective of conservative, endovascular or surgical treatment. Activity of CAD was stable in these patients and those with acute coronary syndrome (ACS) were excluded. Chronic kidney disease (CKD) covers all the stages of impaired renal function, indicating estimated glomerular filtration rate (eGFR) ≤ 60 ml/min/1.73m2.[5] Patients with atrial fibrillation (AF) due to evident rheumatic mitral valve diseases, episode of mitral valve replacement or valvuloplasty were excluded. Therefore, AF was nonvalvular. Paroxysmal AF was defined according to the HRS/EHRA/ECAS 2012 Consensus Statement on Catheter and Surgical Ablation of AF.[6] In this Consensus Statement, the concept of permanent AF was considered inappropriate in that patient and physician ceased further attempts to restore and maintain sinus rhythm, whenever this joint decision is made. However, the term of permanent AF, defined as longstanding AF impossible to be terminated by any means, was used in this study in contrast to paroxysmal AF. AF outpatients (n = 33) were followed every month for anticoagulation, i.e., 20 patients showed permanent AF whereas 13 patients had paroxysmal AF. In AF patients treated with warfarin, time in therapeutic range (TTR) of the international normalized ratio of prothrombin time (PT-INR) ranged from 51 to 72% (65.6 ± 0.9%). Dabigatran (n = 7) and rivaroxaban (n = 5) were also prescribed newly or converted from warfarin. Transthoracic echocardiography and Holter monitoring were conducted in all AF patients. Treatment of the aforementioned coronary risk factors was under the discretion of the treating physicians in outpatient clinics. Medication and lifestyle including smoking were not altered in any patient during the study period.

Erythrocyte Filterability

Erythrocyte suspensions were prepared as described elsewhere.[7] In brief, venous blood (approximately 10 ml) was sampled in the morning after an overnight fast. Blood cell counting and hematocrit measurement were performed using a hemocytometer (Ace Counter, FLC-240A, Fukuda Denshi Co. Ltd., Tokyo, Japan). After centrifugation at 1300 x g for 10 min, supernatant was aspirated to replace buffy coat and plasma with HEPES-buffered saline. Intact erythrocytes were then washed three times (800 x g, 600 x g and 500 x g for 10 min each) by re-suspension with HEPES-buffered saline and the final hematocrit of erythrocyte suspension was adjusted to 3.0% to prevent erythrocytes sticking within the filter pores and to reuse the specific filter. These procedures were performed within 2 hours after blood sampling for subsequent filtration experiments.[7]

Erythrocyte filterability (whole cell deformability) was investigated blindly by filtration technique (Model NOBU-II, Tsukasa Sokken Co. Ltd., Tokyo, Japan) as reported elsewhere.[8,9] Nickel mesh filters were produced by a photo-fabrication technique (Dainippon Printing Co. Ltd., Tokyo, Japan) and characterized by regularly distributed pores of identical size and shape (Fig. 1A), which guarantees the sensitivity of filtration experiments even in the erythrocyte suspension with low (3.0%) hematocrit value. A specific filter with appropriate pore size (4.94 μm in diameter) was used repetitively by sonication during a series of experiments to guarantee the reproducibility. The relationship between hydrostatic pressure (P; mmH2O) and time (t; sec) was obtained during continuous filtration under gravity using a pressure transducer. P was transformed to the height of the meniscus in the vertical tube (h; mm) and flow rate (Q; ml/min) was calculated by the rate of fall of the meniscus ($\Delta h/\Delta t$) and internal cross-sectional area of the vertical tube. P-Q relationship was obtained automatically by software installed on a personal computer (DELL Latitude CS, Dell Inc., Round Rock, TX, USA) and stored simultaneously on Microsoft Office Excel 2003 on Windows XP (Microsoft, Tokyo, Japan). The percentage of Q of erythrocyte suspension relative to Q of saline at 100 mmH2O was used as an index of erythrocyte filterability. Temperature of the specimens was kept at 25°C by circulating isothermal water within a water jacket around the

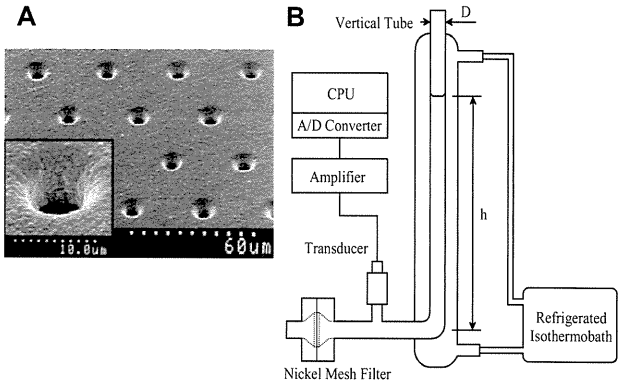

Figure 1: **A: Scanning electron microscopic photograph of a nickel mesh filter. Inset shows magnification of a single pore in this filter. B: Schematic illustration of nickel mesh filtration system. Filtration pressure (P; mmH2O) is converted to the height of the meniscus within the vertical tube (h; mm) using the equation $h = P/\rho g$. Flow rate (Q; ml/min) is calculated using the equation $Q = \pi(D/2)2(\Delta h/\Delta t)$. D, internal diameter of vertical tube; $\Delta h/\Delta t$, first time derivatives of h; g, acceleration of gravity; ρ, specific gravity of specimens.**

vertical tube (Fig. 1B). These examinations were performed at room temperature (22 ± 2°C).

An aliquot of the erythrocyte suspension was fixed with isotonic 1.0% glutaraldehyde solution containing 24.5 mM NaCl and 50 mM phosphate buffer (pH 7.4). Thereafter, the shape of erythrocytes was observed blindly using a differential interference contrast microscope (Diaphoto 300, Nikon Co. Ltd., Tokyo, Japan) at 400 x magnification.

Data Analyses

All data are expressed as means ± SEM. For statistical analyses, human sample size was chosen to provide 90% power with an α error of 0.05. A total of ≥ 310 cases was required provided that the significant intergroup difference of human erythrocyte filterability investigated by this technique is 1.0%.[9] Continuous variables were compared with unpaired Student's t test or Mann-Whitney U test. Erythrocyte filterability (%) was compared by the latter, because Kolmogorov-Smirnov test confirmed that this was not normally distributed ($p < 0.001$). Discrete variables were analyzed by Fisher's exact test or Pearson's $\chi 2$ test. Linear regression was fitted by the standard least square method. Significant contributors to erythrocyte filterability impairment were determined by stepwise multiple regression analysis. None of the variables with missing data qualified. The criteria for entering into the regression model were significant partial correlation coefficient (r) to the filterability, greatest r among the same category even if it was not significant, or otherwise clinically meaningful variables. These analyses were performed using Predictive Analytics Software (PASW) 18.0 version for Windows (SPSS, Inc., IBM, Chicago, IL, USA). Differences with two-sided $p < 0.05$ were considered significant.

Results

Patients' Profile

Baseline characteristics of enrolled subjects are detailed in Table 1. Averages of some listed variables had already reached the upper limit of normal range (systolic blood pressure) or even exceeded the ranges (HbA1c, fasting serum glucose, triglyceride). None of these patients had experienced an episode of evident heart failure (NYHA class ≥III). In patients with CAD, 25 patients had a history of old myocardial infarction and the remaining 23 patients showed stable angina pectoris. Percutaneous coronary intervention (PCI) was performed in 38 patients, and coronary artery bypass grafting surgery (CABG) was conducted in 21 patients. Medication included Ca antagonists (n = 46, 14%), statins (n = 34, 11%), angiotensin receptor blockers (n = 28, 9%), antiplatelet agents (n = 27, 8%), β-blockers (n = 18, 6%), angiotensin converting enzyme inhibitors (n = 16, 5%) and do on.

Table 1: Baseline Characteristics of Subjects (N = 320)

Variables	Means ± SEM	Variables	Means ± SEM
Age (years)	61.5 ± 0.7	LDL cholesterol (mg/dl)	120 ± 2
Body weight (kg)	62.6 ± 0.7	Triglyceride (mg/dl)	160 ± 8
Fat (%)	27.2 ± 0.5	WBC (x 102/μl)	60.2 ± 1.1
BMI (kg/m2)	24.2 ± 0.2	RBC (x 104/μl)	442 ± 3
SBP (mmHg)	140 ± 1	Hb (g/dl)	14.1 ± 0.1
DBP (mmHg)	80 ± 1	Ht (%)	40.9 ± 0.3
HbA1c (%)	7.0 ± 0.1	MCH (pg)	31.9 ± 0.1
FSG (mg/dl)	149 ± 3	MCV (fl)	92.7 ± 0.3
Total Cholesterol (mg/dl)	208 ± 2	MCHC (g/dl)	34.4 ± 0.1
HDL cholesterol (mg/dl)	56 ± 1	Erythrocyte filterability (%)	87.6 ± 0.2

BMI, body mass index; DBP, diastolic blood pressure; FSG, fasting serum glucose; MCH, mean corpuscular hemoglobin; MCHC, mean corpuscular hemoglobin concentration; MCV, mean corpuscular volume; SBP, systolic blood pressure.

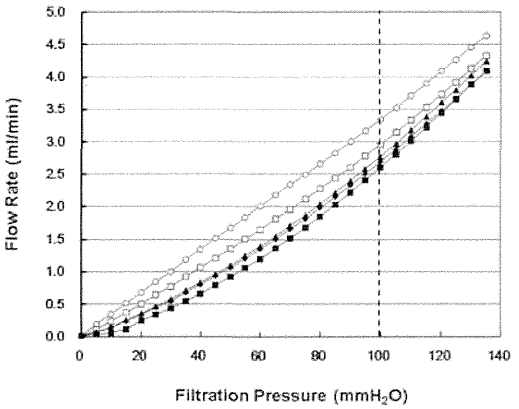

Figure 2A: A: Representative P-Q relationships during continuous filtration experiment using erythrocyte suspensions and HEPES-buffered saline. The P-Q relationships with open symbols correspond to filtrations of saline (open circles) or erythrocyte suspension obtained from a healthy non-smoker without coronary risk factors (open squares). Closed symbols indicate representative patients with diabetes (closed triangles), dyslipidemia (closed diamonds) and permanent atrial fibrillation (closed squares). Q in patients with these diseases (closed symbols) is less than Q in a subject without them (open squares) at any given P. B: Magnification of the P-Q curves at filtration pressure around 100 mmH20.

Representative Filtration Data

Hematologically, there were no remarkable erythrocytes shape changes observed in the enrolled subjects. Figure 2 shows representative results of the nickel mesh filtration experiments. The continuous filtration process yielded P-Q relationships for control

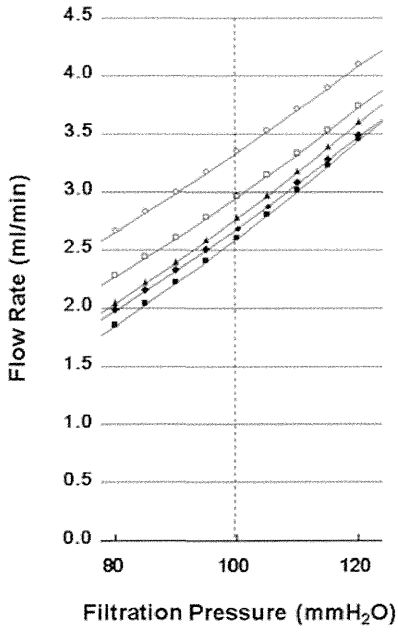

Figure 2B: B: Magnification of the P-Q curves at filtration pressure around 100 mmH20.

Table 2: Correlation of Categorical Factors and Erythrocyte Filterability

Factors		n	Erythrocyte filterability (%)	p
Gender	male	209	87.4 ± 0.2	
	female	111	88.0 ± 0.3	0.072
Current Smoking	(−)	201	87.9 ± 0.2	
	(+)	119	87.2 ± 0.3	0.059
Hypertension	(−)	213	87.6 ± 0.2	
	(+)	107	87.8 ± 0.3	0.867
Dyslipidemia	(−)	217	87.6 ± 0.2	
	(+)	103	87.7 ± 0.3	0.841
Atrial fibrillation	(−)	287	87.8 ± 0.2	
	(+)	33	86.3 ± 0.9	0.308
Diabetes mellitus	(−)	100	88.1 ± 0.2	
	(+)	220	87.4 ± 0.2	0.200
CKD	(−)	184	87.9 ± 0.2	
	(+)	136	87.2 ± 0.3	0.041
CAD	(−)	272	88.2 ± 0.2	
	(+)	48	87.5 ± 0.3	0.407

Erythrocyte filterability is expressed as mean ± SEM. CAD, coronary artery disease; CKD, chronic kidney disease;
n, number of subjects in a specific group; p, probability.

saline and erythrocyte suspensions. Reproducibility of the filtration experiment was confirmed in that P-Q curves obtained by filtration of the same specimen were superimposable as in our recent study.[8,9] Saline demonstrated a linear P-Q relationship passing through the origin, which is compatible with Newtonian fluid. P-Q relationships for the erythrocyte suspensions displayed smooth and upward concave curves over the low-pressure region. These findings indicate that erythrocyte suspension shows non-Newtonian behavior, which is evident under a low-shear-rate condition. Open squares correspond to erythrocyte suspensions obtained from subjects without any coronary risk factors. Closed symbols indicate those obtained from patients with at least one risk factor. Q of erythrocyte suspensions obtained from patients with these risk factors were always less than Q in patients without them at any given pressure. These findings indicate that these coronary risk factors impair the human erythrocyte filterability.

Table 3: Correlation of Continuous Variables and Erythrocyte Filterability

	(N = 320)	
Variables	r	p
Age (years)	0.041	0.460
Body weight (kg)	−0.130	0.020
BMI (kg/m2)	−0.094	0.095
Fat (%)	−0.074	0.293
SBP (mmHg)	−0.033	0.557
DBP (mmHg)	−0.027	0.639
HbA1c (%)	−0.137	0.014
Total cholesterol (mg/dl)	−0.062	0.271
HDL cholesterol (mg/dl)	0.100	0.076
LDL cholesterol (mg/dl)	−0.101	0.073
Triglyceride (mg/dl)	−0.159	0.004
MCH (pg)	−0.014	0.798
MCV (fl)	−0.018	0.742
MCHC (g/dl)	0.003	0.954

,p, probability; r, partial correlation coefficient. Other abbreviations are the same as in Table 1.

Erythrocyte Filterability and Coronary Risk Factors

Relationships between categorical factors and erythrocyte filterability are shown in Table 2. CKD alone showed significant impairment of erythrocyte filterability (p = 0.041). The filterability in AF patients did not differ from that in the remaining subjects, and the filterability in permanent AF was equivalent to that in paroxysmal AF. Correlations of continuous variables and erythrocyte filterability are demonstrated in Table 3. Body weight, HbA1c and triglyceride showed significant inverse correlation, whereas hematological parameters relating to erythrocyte size (mean corpuscular volume; MCV) and internal density (mean corpuscular hemoglobin concentration; MCHC) did not show any correlation with filterability.

Prior to the multiple regression analysis, demographic variables suitable for inclusion into the regression model were selected. For categorical variables, CKD was selected for significance (p = 0.041), current smoking was included as a potent risk of hemorheology,10 and AF was selected as an outcome of overall risk accumulation.6 For continuous variables, body mass index (BMI, p = 0.095) instead of body weight (p = 0.020) was selected as a surrogate of obesity. HbA1c (p = 0.014) and triglyceride (p = 0.004) were selected for respective significance. Although hematological indices were not significant, MCV was selected for its greatest r.

Multiple regression analysis was performed to identify significant covariates contributing to the impairment of erythrocyte filterability with concurrent avoidance of multi-colinearity by monitoring the variance inflation factors. Table 4 shows five regression models including selected continuous or categorical variables according to stepwise reduction. Multiple correlation coefficients were highly significant in this series of regression models. AF was the greatest contributor to the impaired erythrocyte filterability in all the listed models with high significance (p = 0.002 - 0.023).

Erythrocyte filterability of AF patients did not differ from that of the remaining patients (Table 2). However, AF remained alone as the greatest contributor to the impaired erythrocyte filterability (Table 4). Table 5 shows the distribution of AF in patients with coronary risk factors. AF was prevalent significantly (p < 0.001) in hypertensive and dyslipidemic patients. Table 6 further indicates the effects of coronary risk accumulation on the erythrocyte filterability. Multiple comparison of the filterability under the stepwise accumulation of coronary risk factors showed highly significance (p < 0.001), i.e., the erythrocyte filterability was impaired synergistically during the accumulation of coronary risk factors in addition to AF. However, the filterability was not different with respect to the types of CAD (old myocardial infarction vs. stable angina), modality of treatment (PCI vs. CABG), and choice of medication (not shown).

Discussion

Main Findings

The erythrocyte deformability has significant impact on the apparent blood viscosity, which has profound influence on the coronary blood flow,2 development of myocardial infarction and the resultant infarct size.[11] However, the involvement of abnormal erythrocyte behaviors